Int. J. Electrochem. Sci., 16 **(2021)** Article ID: 210566, doi: 10.20964/2021.05.02

International Journal of
ELECTROCHEMICAL
SCIENCE
www.electrochemsci.org

Short Communication

Electric Properties of Deformable Rubber/CNTs/*p*-Si Composites under Pressure

Muhammad Tariq Saeed Chani[1,2*], *Khasan S. Karimov*[3,4], *Hadi M. Marwani*[1,2], *Mohammed M. Rahman*[1,2], *Abdullah M. Asiri*[1,2]

[1] Center of Excellence for Advanced Materials Research, King Abdulaziz University, Jeddah 21589, P.O. Box 80203, Saudi Arabia
[2] Chemistry Department, Faculty of Science, King Abdulaziz University, Jeddah 21589, P.O. Box 80203, Saudi Arabia
[3] Ghulam Ishaq Khan Institute of Engineering Sciences and Technology, Topi-23640, KPK, Pakistan
[4] Center for Innovative Development of Science and Technologies of Academy of Sciences, Rudaki Ave., 33, Dushanbe, 734025, Tajikistan
[*]E-mail: mtmohamad@kau.edu.sa, tariqchani1@gmail.com

Received: 29 October 2020 / *Accepted:* 31 January 2021 / *Published:* 31 March 2021

Rubbing-in technology was used to fabricate the deformable CNT-*p*-Si-rubber nanocomposites. The effect of uniaxial compressive displacement (up to ~ 6% of the length of samples) and uniaxial pressure (up to 0.12 kgf/cm^2) on the I-V characteristics of the samples were investigated. It was obtained that the I-V characteristics under the effect of displacement or pressure are shifted toward increasing currents at permanent applied voltages. The nonlinearity coefficients of the I-V characteristics slightly reduced due to displacement or pressure and increased with applied voltage. It was observed that the investigated composite samples' resistances crucially decreased with increase in compressive displacement or pressure. It may be, first of all, due to the decrease in distances between CNT particles in the composite under compression or pressure and the increase in the cross-section area of the samples, accordingly. The composite samples can be used as deformable and shocked-proof pressure and displacement sensors.

Keywords: rubbing-in technology, displacement, uniaxial pressure, non-linearity

1. INTRODUCTION

Current-Voltage (I-V) characteristics of the different kinds electronic devices shows indirectly the electro physical processes, namely charges transfer and generation, that take place in the materials under applied voltage. It means investigation of the I-V characteristics are important for understanding of the properties of materials and for application in practice concerned devices as non-liner resistors

and diodes. The electrical characteristics of chemically grown self-aligned carbon nanotubes were investigated by measurements of the I-V characteristics in Ref. [1] and it was found that the samples showed field emission properties which depend upon the diameter lithographic gate aperture to grow the CNTs. The numerical-modeling of the I-V characteristics of CNTs-based field effect transistors was presented in Ref. [2]. Temperature dependences of I-V of CNT-based *n*-*i*-*n*-MOSFET and *p*-*i*-*n*-TFET were studied in Ref. [3].

For the understanding of devices, I-V characteristics the structure and physical properties of the materials which were used for fabrication of the devices should be investigated. In this concerns it can be mentioned a number of published papers where transport properties (electrical) of isolated Schottky diodes (CNTs/Si heterojunction) [4], strain sensing electrical conductivity CNTs-graphene–rubber composite under cycling loading [5], physical properties and variability in output characteristics of SWCNTs thin-film transistors [6] were investigated.

The composites of Si_3N_4 with various amounts (1, 3 or 5 wt.%) of CNTs were prepared by hot pressing (isostatic) and investigated [7]. It was observed that the Si_3N_4 matrices' electrical properties essentially changed with CNTs. The effect of CNTs' 1-octadecanol (C_{18}) functionalization on natural rubber-CNTs (NR-CNTs) composites' electrical properties were studied [8]. Stress–strain data revealed that C_{18} functionalization increased the tensile strength of the NR-CNTs composite. In [9] it was described the synthesis of SWCNT/Si rubber composites for compliant electrodes' fabrication.

Recently, in continuation of our efforts for the development of sensing devices [10-24] we investigated graphene and CNTs powder based multifunctional displacement, pressure and temperature sensors [16], graphene and orange dye solid electrolyte cells for humidity sensing [25] and graphene-rubber nanocomposite based multifunctional flexible sensors [15]. In persistence of our efforts in the investigation of the deformable composites' properties and devices in this paper we are presenting data on influence of the compressive displacement and pressure on the I-V characteristics of deformable samples based on rubber-CNT-*p*-Si composites.

2. EXPERIMENTAL

The CNTs (carbon nanotubes) powder and *p*-Si wafer were purchased from Sigma Aldrich and Sun Nanotek Co. LTD (http://www.sunnano.com), respectively. The 100 to 200 nm long multiwalled carbon nanotubes had 10 to 30 nm diameter. By ball milling the Si wafer was converted to Si powder with particle size ranging from 9 µm to 12 µm. The rubbing-in technology was used to fabricate the sensors. For sensor fabrication the rubber substrates were fixed on the solid platform at room temperature and the metallic blocks were used to penetrate the powders into the substrates. Figure 1a illustrates the rubbing-in technology. The detail description of the process is given in ref. [15]. Initially the rubber-CNTs composite layers were fabricated on the deformable rubber substrates by rubbing the CNT powder on the substrates using rubbing-in technique. After that in the middle of rubber-CNTs layers a gap was made up to pure rubber level. This gap was filled by composite of CNT-p-Si powders (50%:50% by weight), which was prepared by mixing both powders using mortar and pestle. By rubbing-in the mixture of CNT and p-Si powders were built-in rubber substrate's gap. Resultantly the

rubber-CNT-p-Si composite was formed. All the samples were fabricated at pressure of 50 g/cm^2. The schematic diagrams shown in Fig. 1b and 1c represent front and top views of the fabricated samples, respectively. The rubber-CNT-*p*-Si composite played a role of sensitive material.

X-Ray Diffraction analysis (XRD) was performed to characterize the rubber-CNTs-p-Si composite. X-ray diffraction of the samples were conducted on Philips PW1830 X-ray diffraction system in Bragg-Brentano (θ-2θ) scan mode using Cu-Kα radiation source at room temperature. Each sample was run three times to achieve reproducible results. For I-V characteristics the current and voltages were measured using DT-4253 digital multi-meters. All experiments were conducted at room temperature conditions. The uniaxial compressive displacements or pressures were applied along the length of the rectangular prism samples by using micrometer mechanism or weights in special experimental arrangement. The processes of application of forces on the rubber sample are shown also in Fig.1c.

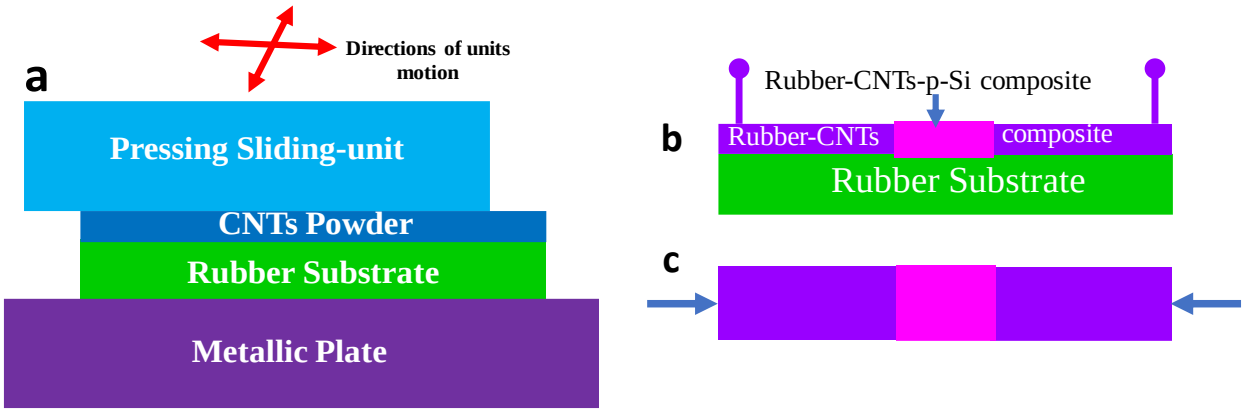

Figure 1. Schematic illustrations of (a) the rubbing-in technology to form rubber-CNTs-p-Si composite, the front view (b) and top view (c) of the built-in rubber-CNTs-*p*-Si composite for the investigation of I-V characteristics.

3. RESULTS AND DISCUSSION

The XRD spectra of rubber, *p*-silicon, CNT and rubber/CNT/p-silicon composite are shown in Fig.2. The rubber's pattern shows high intensity peaks (Bragg's diffraction) at 2θ of 36°, 29.4° and 23.1°. These peaks are attributed to highly ordered polyvinyl chloride chains [26]. The CNTs spectrum contains major peak at 26.2° (002) that corresponds to hexagonal graphite which is highly conductive. This peak (at 26.2°) is similar to standard XRD data (ICSD code: 031170). The peak at 38.4° corresponds to functional group attached with CNTs. A broad peak of CNTs consistent with other studies [27] was also observed at 2θ of 44.3° (101). A sharp peak of *p*-type silicon powder [28] was observed at 2θ = 68.9°. The XRD spectrum of rubber/CNT/p-silicon composite contains all above discussed peaks.

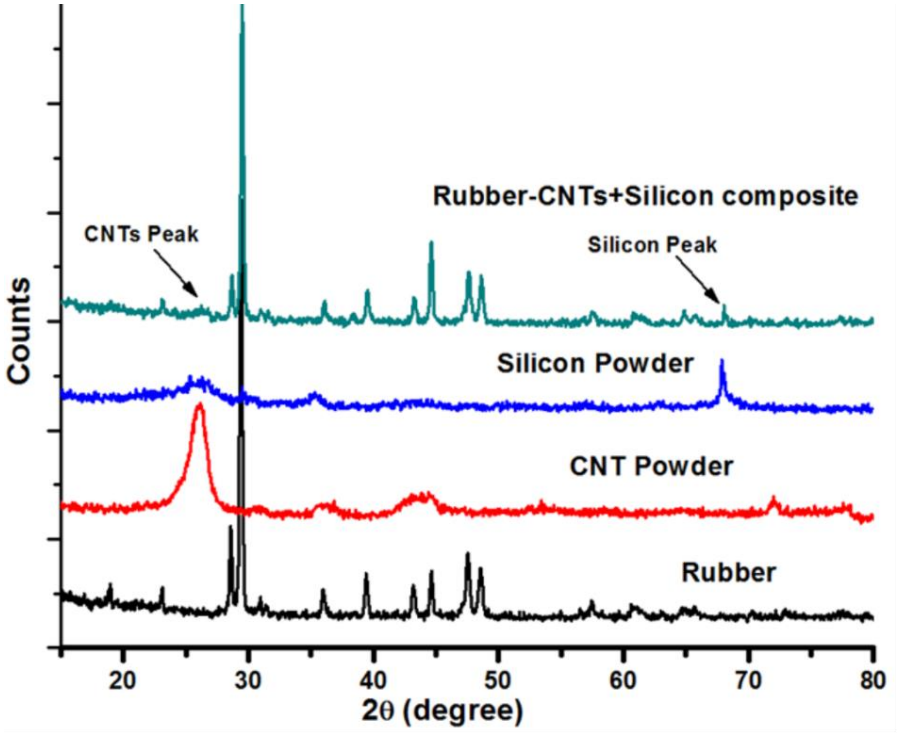

Figure 2. XRD-spectra of rubber, CNTs powder, silicon powder and rubber-CNTs-*p*-Si composite

Figure 3 shows I-V characteristics of the rubber-CNTs-*p*-Si composite samples measured at different values of compressive displacements. It is seen that as displacement increased the current through the sample also increased. On increasing compressive displacement from 0 to 800 μm the current increases from 8 μA to 76 μA. The I-V characteristics are super-linear.

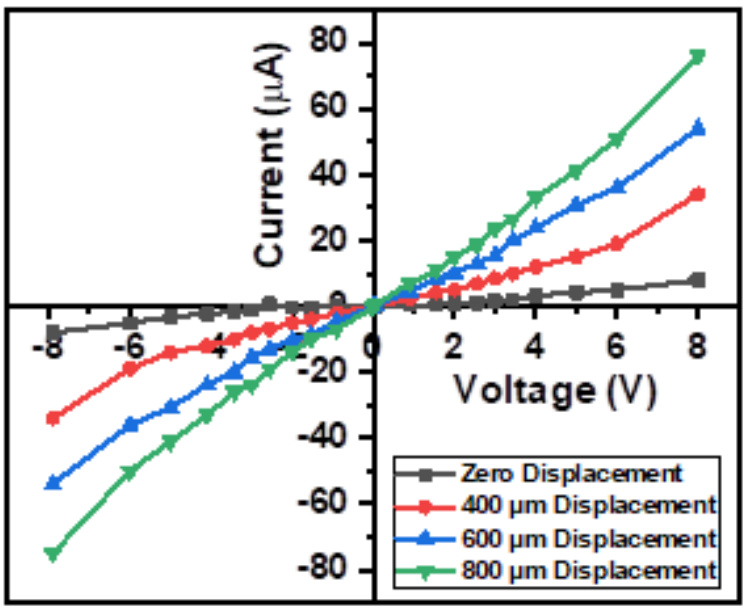

Figure 3. I-V characteristics of the CNT-p-Si-rubber composite sample at various compressive displacements

The non-linearity coefficient of the I-V characteristics can be determined by the following expression:

$$\beta = dI\ V_o / I_o\ dV \quad (2)$$

Figure 4 shows β (V) relationships accordingly for rubber-CNT-*p*-Si composite sample at zero displacement and at displacement equal to 800 μm. It is seen that for the rubber-CNT-*p*-Si composite sample non-linearity coefficient (β) is in the range of (1.2-1.8) at zero displacement and is equal to (1.1-1.7) at displacement of 800 μm.

Non-linearity of I-V characteristics can be observed, first of all, due to metal-semiconductor contact properties, namely, Schottky junction properties [29-32]. Secondly, due to particular properties of semiconductor, as active materials, in our case CNT-p-Si-rubber composite: the conductivity of the composite can be increased due to heating by current in some extend due to presence of p-Si. And finally, it can be considered that non-linearity of the I-V characteristics, partly, may be due to electric field effect. Further investigations are needed to make more concrete decision concerning non-linearity of I-V characteristics.

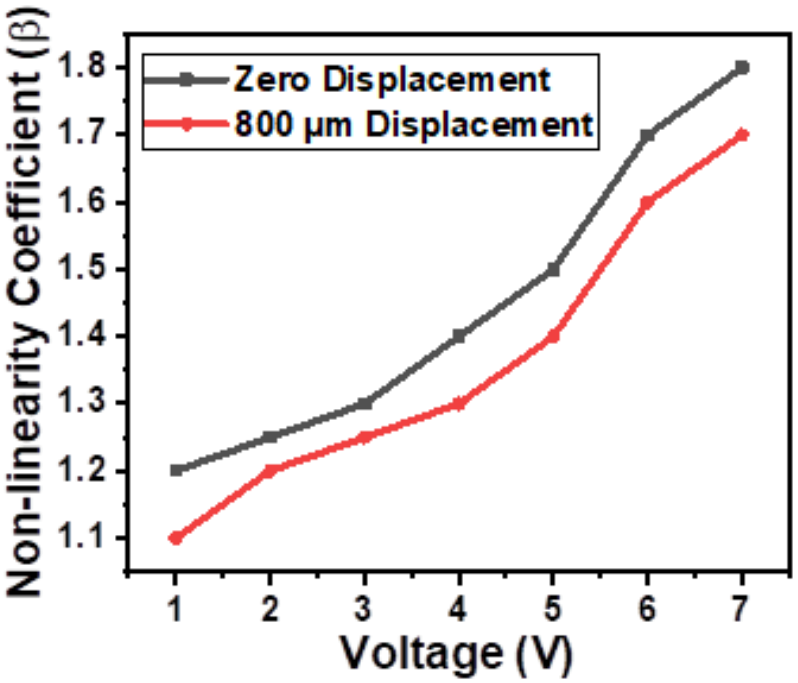

Figure 4. β (V) relationships for CNT-p-Si-rubber composite sample at zero displacement and at displacement equal to 800 μm.

Figure 5 shows I-V characteristics of the rubber-CNT-*p*-Si composite sample at different uniaxial pressures. It can be seen that as the uniaxial pressure increased the current through the sample increased. On increasing pressure from 0 to 0.12 kf/cm2 the passing through sample increased from 7.5 μA to 15.0 μA. It is also seen that the characteristics are sub-linear.

Increase of the current due to compressive displacement or pressure may be due to decrease of the resistance of the samples due to decrease of the inter particles (first of all CNT particles) distance and increase of the cross-section area under compression.

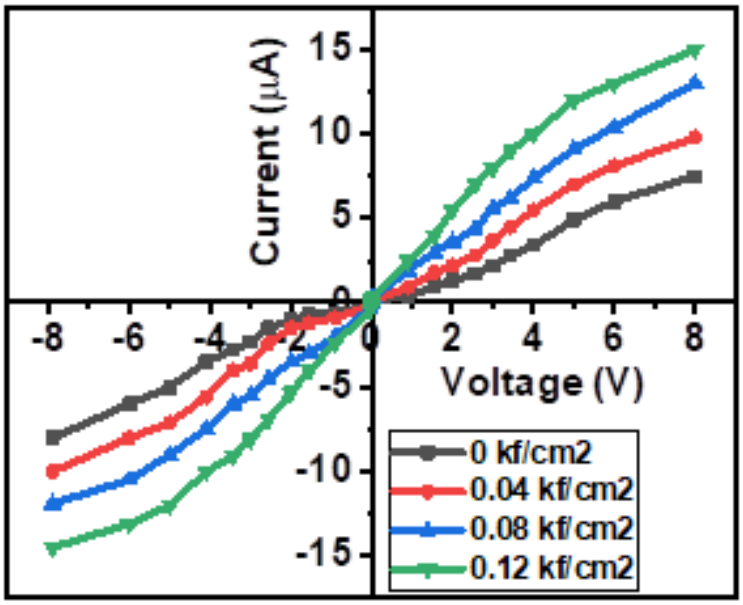

Figure 5. I-V characteristics of the CNT-p-Si-rubber composite sample at different uniaxial pressures

4. CONCLUSIONS

As is known at present flexible, stretchable or deformable electronics are popular and therefore the new material synthesis, mechanical design, and fabrication strategies are developing [33-35], including stretchable heaters, energy convertors, storage devices, transistors and sensors. We hope that the paper presented by us about the I-V characteristics of elastic deformable rubber-CNTs-*p*-Si composite under compression and pressure will be useful for researchers, designers and manufacturers of the flexible and stretchable electronic devices as well.

ACKNOWLEDGEMENTS
This project was funded by the Deanship of Scientific Research (DSR), King Abdulaziz University, Jeddah, Saudi Arabia under grant no. (KEP-13-130-41). The authors, therefore, acknowledge with thanks DSR technical and financial support.

References

1. G. Pirio, P. Legagneux, D. Pribat, K. Teo, M. Chhowalla, G. Amaratunga and W. Milne, *Nanotechnol.*, 13 (2001) 1.
2. J.M. Marulanda, A. Srivastava and S. Yellampalli, in *2008 40th Southeastern Symposium on System Theory (SSST)*, IEEE, (2008) 235-238.

3. S.G. Shirazi, G. Karimi and S. Mirzakuchaki, *ECS J. Solid State Sci. Technol.*, 5 (2016) M44-M50.
4. T. Uchino, F. Shimpo, T. Kawashima, G. Ayre, D. Smith, C. de Groot and P. Ashburn, *Appl. Phys. Lett.*, 103 (2013) 193111.
5. H. Yang, X. Yao, L. Yuan, L. Gong and Y. Liu, *Nanoscale*, 11 (2019) 578-586.
6. J. Chen and S. Kumar, *IEEE Trans. Nanotechnol.*, 17 (2018) 353-361.
7. C. Balázsi, B. Fényi, N. Hegman, Z. Kövér, F. Wéber, Z. Vértesy, Z. Kónya, I. Kiricsi, L.P. Biró and P. Arató, *Composites Part B,* 37 (2006) 418-424.
8. P.S. Thomas, A.A. Abdullateef, M.A. Al-Harthi, M.A. Atieh, S. De, M. Rahaman, T. Chaki, D. Khastgir and S. Bandyopadhyay, *J. Mater. Sci.*, 47 (2012) 3344-3349.
9. T.A. Kim, H.S. Kim, S.S. Lee and M. Park, *Carbon*, 50 (2012) 444-449.
10. M. Chani, K.S. Karimov, K.S. KARIMOV, J.-U. NABI, A. AHMED, I. KIRAN and A. ASIRI, *J. Optoelectron. Adv. Mater.*, 21 (2019) 588-593.
11. M.T.S. Chani, K.S. Karimov and A.M. Asiri, *Semicond.*, 53 (2019) 1622-1629.
12. M.T.S. Chani, K.S. Karimov, A.M. Asiri, N. Ahmed, M.M. Bashir, S.B. Khan, M.A. Rub and N. Azum, *PLoS One*, 9 (2014) e95287.
13. M.T.S. Chani, K.S. Karimov, J.-u. Nabi, M. Hashim, I. Kiran and A.M. Asiri, *Int. J. Electrochem. Sci*, 13 (2018) 11777-11786.
14. M.T.S. Chani, S.B. Khan, A.M. Asiri, K.S. Karimov and M.A. Rub, *J. Taiwan Inst. Chem. Eng.*, 52 (2015) 93-99.
15. M.T.S. Chani, K.S. Karimov, E.M. Bukhsh and A.M. Asiri, *Int. J. Electrochem. Sci*, 15 (2020) 5076-5088.
16. M.T.S. Chani, K.S. Karimov and A.M. Asiri, *Semicond.*, 54 (2020) 85-90.
17. M.T.S. Chani, K.S. Karimov, S.B. Khan, N. Fatima and A.M. Asiri, *Ceram. Int.*, 45 (2019) 10565-10571.
18. M.T.S. Chani, K.S. Karimov and A.M. Asiri, *J. Mater. Sci. Mater. Electron.*, 30 (2019) 6419-6429.
19. M.T.S. Chani, *Microchim. Acta*, 184 (2017) 2349-2356.
20. A.M. Asiri and M.T.S. Chani, US 10317356, USA, (2019).
21. M. Tariq Saeed Chani, S. Bahadar Khan, A. M Asiri, G. Saeed and M. Nadeem Arshad, *Curr. Nanosci.*, 12 (2016) 564-568.
22. M.T.S. Chani, S.B. Khan, K.S. Karimov, M. Abid, A.M. Asiri and K. Akhtar, *J. Semicond.*, 36 (2015) 023002.
23. M.T.S. Chani, K.S. Karimov, F. Khalid, S. Abbas and M. Bhatty, *Chin. Phys. B*, 22 (2013) 010701.
24. M.T.S. Chani, K.S. Karimov, F.A. Khalid, K. Raza, M.U. Farooq and Q. Zafar, *Physica E*, 45 (2012) 77-81.
25. M.T.S. Chani, K.S. Karimov, H. Meng, K.M. Akhmedov, I. Murtaza, U. Asghar, S.Z. Abbass, R. Ali, A.M. Asiri and N. Nawaz, *Russ. J. Electrochem.*, 55 (2019) 1391-1396.
26. I.P. Ejidike, C.W. Dikio, D. Wankasi, E.D. Dikio and F.M. Mtunzi, *Int. J. Environ. Stud.*, 75 (2018) 932-949.
27. Y. Lu, X. Liu, W. Wang, J. Cheng, H. Yan, C. Tang, J.-K. Kim and Y. Luo, *Sci. Rep.*, 5 (2015) 16584.
28. T.T.K. Chi, N.T. Le, B.T.T. Hien, D.Q. Trung and N.Q. Liem, *Commun. Phys.*, 26 (2016) 261-268.
29. C.-C. Hsieh, Y.-F. Chang, Y.-C. Chen, D. Shahrjerdi and S.K. Banerjee, *ECS J. Solid State Sci. Technol.*, 6 (2017) N143-N147.
30. M. Egashira, Y. Shimizu, Y. Takao and Y. Fukuyama, in *Proceedings of the International Solid-State Sensors and Actuators Conference - TRANSDUCERS '95*, (1995) 718-721.
31. T. Taniguchi, J. Tanaka, O. Mishima, T. Ohsawa and S. Yamaoka, *Diamond Relat. Mater.*, 2

(1993) 1473-1478.
32. S. Jagtap, S. Rane, S. Gosavi and D. Amalnerkar, *Microelectron. Eng.*, 88 (2011) 82-86.
33. T.S. Natarajan, S.B. Eshwaran, K.W. Stöckelhuber, S. Wießner, P. Pötschke, G. Heinrich and A. Das, *ACS Appl. Mater. Interfaces*, 9 (2017) 4860-4872.
34. A.S. Fiorillo, C.D. Critello and S.A. Pullano, *Sens. Actuators A*, 281 (2018) 156-175.
35. S. Liu, V.S. Chevali, Z. Xu, D. Hui and H. Wang, *Composites Part B*, 136 (2018) 197-214.